doi:10.1038/nature14448

New species from Ethiopia further expands Middle Pliocene hominin diversity

Yohannes Haile-Selassie[1,2], Luis Gibert[3], Stephanie M. Melillo[4], Timothy M. Ryan[5], Mulugeta Alene[6], Alan Deino[7], Naomi E. Levin[8], Gary Scott[7] & Beverly Z. Saylor[2]

Middle Pliocene hominin species diversity has been a subject of debate over the past two decades, particularly after the naming of *Australopithecus bahrelghazali* and *Kenyanthropus platyops* in addition to the well-known species *Australopithecus afarensis*. Further analyses continue to support the proposal that several hominin species co-existed during this time period. Here we recognize a new hominin species (*Australopithecus deyiremeda* sp. nov.) from 3.3–3.5-million-year-old deposits in the Woranso–Mille study area, central Afar, Ethiopia. The new species from Woranso–Mille shows that there were at least two contemporaneous hominin species living in the Afar region of Ethiopia between 3.3 and 3.5 million years ago, and further confirms early hominin taxonomic diversity in eastern Africa during the Middle Pliocene epoch. The morphology of *Au. deyiremeda* also reinforces concerns related to dentognathic (that is, jaws and teeth) homoplasy in Plio–Pleistocene hominins, and shows that some dentognathic features traditionally associated with *Paranthropus* and *Homo* appeared in the fossil record earlier than previously thought.

Recent fossil hominin discoveries from eastern and central Africa have been described as indicating the existence of multiple locomotor adaptations[1] and taxonomic diversity[2–5] during the Middle Pliocene. Notably, *Kenyanthropus platyops* from Kenya and *Australopithecus bahrelghazali* from Chad were argued to be morphologically distinct from the contemporaneous *Au. afarensis*[2–5]. Concerns have been raised about the validity of these two taxa, either because identification was based largely on a single specimen or because the type specimen was heavily distorted[6]. Yet further studies addressing these concerns maintain the initial proposal of taxonomic diversity[4,5]. More recently, we described a 3.4-million-year (Myr)-old partial foot (BRT-VP-2/73) from the Burtele area of Woranso–Mille, Ethiopia[1]. The specimen is contemporaneous with *Au. afarensis*, but demonstrates the existence of a distinct mode of bipedal locomotion. The BRT-VP-2/73 foot combines a grasping hallux with lateral rays that exhibit adaptation to hyperdorsiflexion at the metatarsophalangeal joint, similar to the morphology described for *Ardipithecus ramidus*[7]. This specimen was not assigned to any taxon, pending the recovery of cranial and dentognathic fossils from the same geographic and stratigraphic vicinity. Continued fieldwork in the Burtele area has resulted in the recovery of new dentognathic fossil remains, including partial and complete mandibles, a partial maxilla with dentition, and few isolated teeth (Table 1). Unfortunately, none of them is clearly associated with BRT-VP-2/73 (see Supplementary Note 1 for details).

The new remains described here show clear similarities with *Australopithecus* and lack the diagnostic features of *Ardipithecus*, *Paranthropus*, *Kenyanthropus* and *Homo*. Various aspects of dentognathic morphology distinguish these specimens from the contemporaneous *Au. afarensis* and warrant their assignment to a new species (Fig. 1).

Order Primates Linnaeus, 1758
Suborder Anthropoidea Mivart, 1864
Superfamily Hominoidea Gray, 1825
Genus *Australopithecus* Dart, 1925
Australopithecus deyiremeda sp. nov.

Etymology. From the local Afar language terms *deyi*, meaning close, and *remeda*, meaning relative; thus referring to the species being a close relative of all later hominins.

Holotype. The holotype is BRT-VP-3/1 (Fig. 1a–e), a left maxilla with upper second incisor–upper second molar (I^2–M^2) found by M. Barao on 4 March 2011. The originals of the holotype and paratypes are housed at the Paleoanthropology Laboratory of the National Museum of Ethiopia, Addis Ababa.

Paratypes. The paratypes are BRT-VP-3/14 (Fig. 1f–h), a complete mandible corpus with the apical halves of left lower incisor–right lower incisor (LI_2–RI_2) and crowns of right lower premolar–lower molar (RP_3–M_3), lacking the ascending rami; and WYT-VP-2/10 (Fig. 1i–k), a right edentulous mandible. Both specimens were found by A. Asfaw. Detailed anatomical descriptions, additional images, and measurements are provided in Supplementary Note 2, Extended Data Figs 1 and 2, and Extended Data Tables 1, 2 and 5).

Referred specimen. BRT-VP-3/37 (Fig. 1l–p), a right maxillary fragment with P^4. This specimen was found only 5 m east of BRT-VP-3/14 and both specimens may belong to the same individual. However, this cannot be determined with confidence owing to the fragmentary nature of BRT-VP-3/37.

Localities. The Burtele (BRT) and Waytaleyta (WYT) collection areas are located south of the perennial Mille River and north of the Mille–Chifra road. All localities are situated within an area of 3 km^2 (Fig. 2). The coordinates of the holotype are 11° 27′ 43.9′′ N and 40° 31′ 41.0′′ E (GPS datum WGS84).

Provenience. The holotype and paratypes from BRT-VP-3 are surface finds, weathered out of a sandstone at the bottom of a 6-m thick section of sandstone and siltstone capped by a 2-m thick basaltic flow. A tuff radiometrically dated to 3.469 ± 0.008 (mean ± s.d.) Myr is located approximately 1 m above the basaltic flow. The paratype from WYT-VP-2 was also a surface find, collected from the top of a thin sandstone layer about 15 m above the 3.469-Myr-old tuff. The combined evidence from radiometric, palaeomagnetic and

[1]Cleveland Museum of Natural History, Cleveland, Ohio 44106, USA. [2]Case Western Reserve University, Cleveland, Ohio 44106, USA. [3]University of Barcelona, Martí Franquès s/n, 08028 Barcelona, Spain. [4]Max Plank Institute for Evolutionary Anthropology, Deutscher Platz 6, D-04103 Leipzig, Germany. [5]Pennsylvania State University, University Park, Pennsylvania 16802, USA. [6]Addis Ababa University, PO Box 1176 Addis Ababa, Ethiopia. [7]Berkeley Geochronology Center, 2455 Ridge Road, Berkeley, California 94709, USA. [8]Johns Hopkins University, Baltimore, Maryland 21218, USA.

Table 1 | Fossil hominins from BRT and WYT localities

Specimen number	Preserved elements	Date discovered	Discoverer	Measurements
BRT-VP-1/1	Left M_3 crown fragment	20 February 2006	K. Helem	N/A
BRT-VP-1/2	Left P_4	20 February 2006	K. Helem	10.4 (13.0)
BRT-VP-1/13	Right C_1	20 February 2006	C. Mesfin	9.9, 9.3
BRT-VP-1/18	Left M^2 mesial half	20 February 2006	K. Kayranto	N/A, 13.8
BRT-VP-1/118	Left M_3 fragment	17 February 2012	G. Alemayehu	N/A
BRT-VP-1/120	Left P_4	17 February 2012	A. Elema	9.9, 10.1
BRT-VP-2/10	Frontal fragment	20 February 2006	Y. Haile-Selassie	N/A
BRT-VP-2/73	Right partial foot	15 February 2009	S. Melillo	See ref. [1]
BRT-VP-2/89	Right P^4	17 February 2012	H. Gebreyesus	9.6, 12.9
BRT-VP-2/104	Molar fragment	26 February 2013	M. Mekomeli	N/A
BRT-VP-3/1	Left maxilla (I^2–M^2)	4 March 2011	M. Barao	LI^2, 6.9, 6.6; LC^1, (8.3), (9.4); LP^3, 7.7, 12.0; LP^4, 7.6, 11.8; LM^1, 10.6, 11.0; LM^2, 11.8, 13.2
BRT-VP-3/14	Mandible with dentition	4 March 2011	A. Asfaw	LI_1, 5.4, 8.0; LI_2, 6.5, 9.0; LC_1, 8.0, 10.7; LP_3, 7.6, 10.8; LP_4, 8.2, 10.6; LM_1, (12.6), (12.6); LM_2, (14.8), (13.8); LM_3, (15.8), (13.4)
BRT-VP-3/37	Right maxilla fragment (P^4)	1 March 2013	A. Asfaw	8.2 (12.1)
WYT-VP-2/10	Partial edentulous mandible	5 March 2011	A. Asfaw	N/A

Dental measurements are standard mesiodistal and buccolingual/labiolingual dimensions. Values in parentheses are corrected for breakage or interproximal attrition. All measurements are in millimetres and were taken on the original specimens by the authors. N/A, non-dental specimens and fragments with no measurement.

depositional rate analyses yields estimated minimum and maximum ages of approximately 3.3 and 3.5 Myr, respectively (Fig. 3, Extended Data Fig. 3 and Supplementary Note 3 for details).

Differential diagnosis. *Australopithecus deyiremeda* differs from *Ar. ramidus* by having relatively and absolutely thicker enamel on its molars; a P_4 with three-roots; a robust mandible. It differs from *Au. anamensis* in lacking an extremely receding mandibular symphysis; having a more robust mandibular corpus and a bicuspid P_3. It is distinguished from *Au. afarensis* by its overall mandibular architecture, including the lack of a lateral corpus hollow; low and anteriorly positioned origin of the ascending ramus with pronounced takeoff at the P_4/M_1 level. It also differs in features of the maxilla, including an anteriorly positioned zygomatic origin and in dental size and morphology, specifically an absolutely small upper postcanine dentition and an upper canine that is mesiodistally short and lacks lingual relief. *Australopithecus deyiremeda* differs from *Paranthropus* in lacking molarized premolars and reduced incisors. It is distinguished from *K. platyops* by its transversely convex subnasal region, with incisor alveoli considerably anterior to the bi-canine line; I^1 root larger and more rounded than I^2 root; more prognathic nasoalveolar clivus and

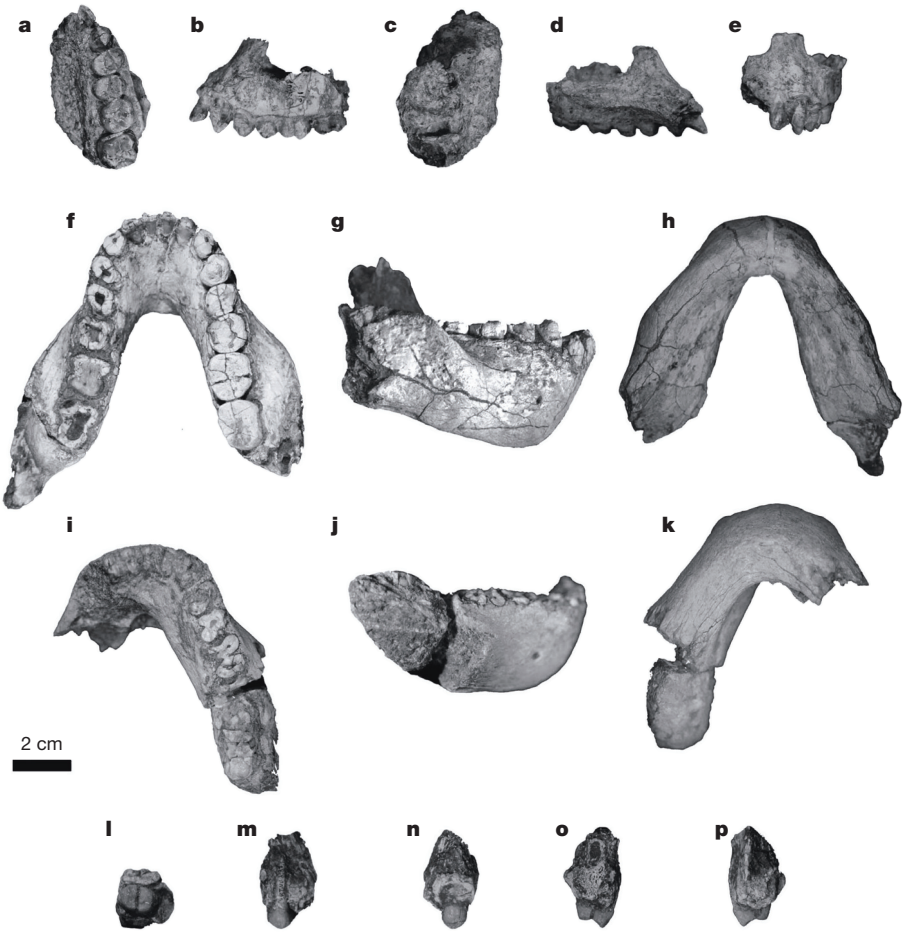

Figure 1 | Holotype BRT-VP-3/1. **a**, Occlusal view. **b**, Lateral view. **c**, Superior view. **d**, Medial view. **e**, Anterior view. Paratype BRT-VP-3/14. **f**, Occlusal view. **g**, Right lateral view. **h**, Basal view. Paratype WYT-VP-2/10. **i**, Occlusal view. **j**, Right lateral view. **k**, Basal view. Referred specimen BRT-VP-3/37. **l**, Occlusal view. **m**, Buccal view. **n**, Lingual view. **o**, Distal view. **p**, Mesial view.

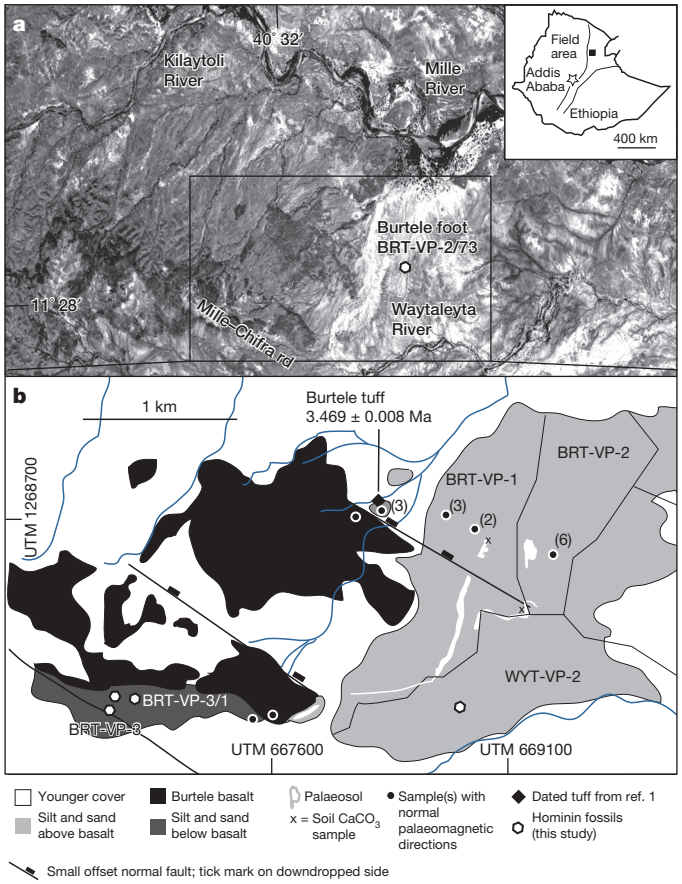

Figure 2 | Location map for the Burtele collection area and the BRT-VP-1, BRT-VP-2, BRT-VP-3 and WYT-VP-2 localities. **a**, Aerial photograph showing the location of the collection area in relation to nearby roads and rivers. **b**, Geological map of the study area showing the outcrop areas of sedimentary and volcanic units and the locations of fossil sites, palaeomagnetic samples (with number of samples indicated in parentheses), the dated Burtele tuff, and location of the holotype and paratypes of *Australopithecus deyiremeda*. The UTM (Universal Transverse Mercator) zone is 37P. The aerial photograph in **a** is reproduced with permission from the Ethiopian Mapping Agency.

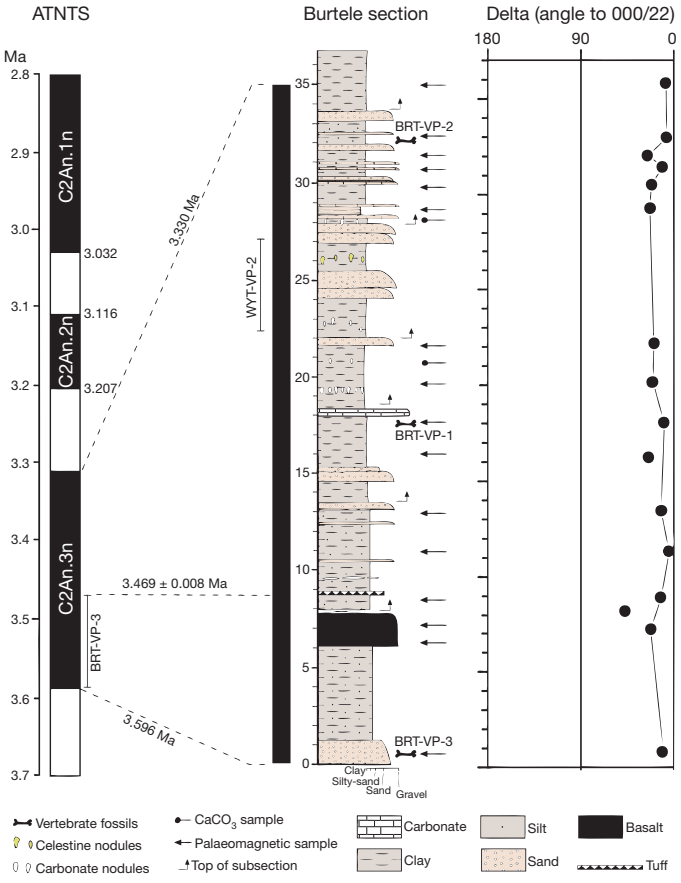

Figure 3 | Palaeomagnetic directions for 16 samples collected from the composite stratigraphic section at Burtele. Directions are shown as the angular distance (delta) to the expected normal direction (000°, 22) for the given latitude. The stratigraphic position of the fossil localities, palaeomagnetic samples and carbonate samples are indicated. All palaeomagnetic samples exhibit normal remanence directions and fall within a single normal magnetozone. K-feldspar phenocrysts from a tuff ~1 m above the basalt have been dated by the $^{40}Ar/^{39}Ar$ method, yielding a mean age of 3.469 ± 0.008 Myr old[1], indicating that this 36-m section corresponds to the normal magnetozone C2An.3n (3.596–3.330 Ma). A minimum sedimentation accumulation rate of 18.6 cm per 1,000 years is calculated for 26 m of strata deposited in the time period <3.33–3.47 Ma. Applying this rate, the fossil locality BRT-VP-3 situated 7 m stratigraphically below the tuff (excluding the 2 m basalt, see Supplementary Note 3) has an estimated age of 3.50–3.47 Myr.

I^2 root obliquely implanted, indicating some degree of procumbency; prominent upper canine and P^3 jugae; presence of incipient canine fossa and weakly expressed zygomaticoalveolar crest. *Australopithecus deyiremeda* can be distinguished from *Au. garhi* by its reduced subnasal prognathism and absolutely smaller canines and postcanine dentition. It differs from early *Homo* by its less incisiform canines, asymmetric P_3, anterior margin of the mandibular ramus arising more anteriorly (opposite distal P_4), mandibular corpus height tapering posteriorly from P_3 to M_3, and by its anterosuperiorly opening mental foramen.

Comparisons

The holotype maxilla (BRT-VP-3/1) has a more anteriorly positioned zygomatic root compared to *Au. anamensis* and most of the known *Au. afarensis* maxillae. However, it overlaps with most early hominins in the degree of subnasal prognathism (as determined by the subnasal angle) and palate depth[3,4,8] (see Extended Data Table 2). Although the position of prosthion on BRT-VP-3/1 cannot be determined with certainty, the maximum estimated subnasal angle of this specimen is ~ 39°, falling within the range of most early hominins but considerably less than the angle reported for KNM-WT 40000, the holotype of *K. platyops* (47°)[4].

The incisive foramen in BRT-VP-3/1 is positioned at the distal bicanine line, whereas in *Au. afarensis* maxillae of comparable size (for example, A.L. 199-1), and early *Homo* specimens such as A.L. 666-1, the foramen is positioned posterior to this line, or at the P^3 level[8]. The palate anterior to the incisive foramen is also flexed inferiorly (see Extended Data Fig. 1i, k, l), a feature considered as derived although it is reported to be variable in *Au. afarensis*[9]. BRT-VP-3/1 shows very little sagittal overlap between the hard palate and the nasoalveolar clivus (3.5 mm) unlike most *Au. afarensis* maxillae (see Extended Data Fig. 4).

Further differences between *Au. deyiremeda* and *Au. afarensis* relate to the morphology of the upper dentition. The cheek teeth of *Au. afarensis* tend to exhibit roughly vertical buccal and lingual walls[10], whereas the buccal and lingual walls of the *Au. deyiremeda* premolars and molars converge occlusally, making the occlusal surface narrower than the base of the crown. The P^3 and P^4 of BRT-VP-3/1 have three roots (Extended Data Fig. 1h, j). This is commonly seen in *Paranthopus* species, but highly variable in *Australopithecus*. *Kenyanthropus platyops* also has three-rooted upper premolars although P^3–P^4 crown morphology is currently unknown for this species[3].

The canine crown of BRT-VP-3/1 is absolutely smaller than almost all known *Australopithecus* upper canines, specifically in its

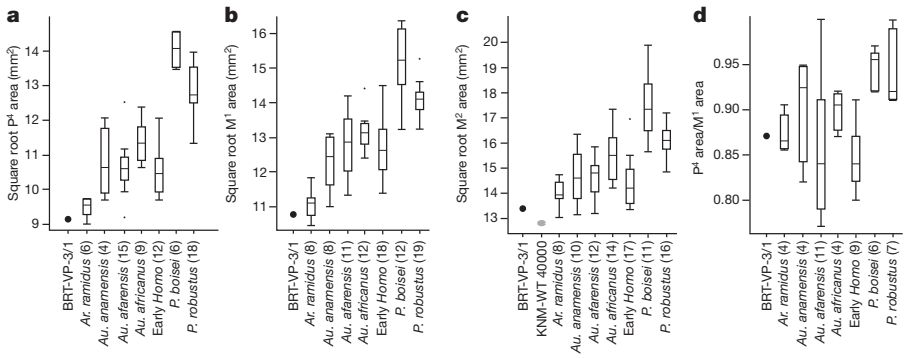

Figure 4 | Box-and-whisker diagrams comparing dental dimensions of the holotype BRT-VP-3/1 with other early hominins. Square roots of P^4–M^2 areas (buccolingual × mesiodistal dimensions) are plotted. The horizontal edges of each box indicate the first quartile (Q_1), the median (Q_2), and the third quartile (Q_3). The superiormost and inferiormost horizontal lines show the maximum and minimum values, respectively, excluding outliers, which are shown above or below these horizontal lines. Metric data for the comparative samples were compiled from refs 9 and 25, 28–33.

mesiodistal dimension, which falls close to the mean of *P. robustus* and *P. boisei* (Extended Data Table 2). It also appears to be long-rooted relative to its crown height, as in *Au. anamensis*[11–13]. Furthermore, the canine of BRT-VP-3/1 does not have pronounced lingual relief and entirely lacks the prominent mesial and distal vertical lingual grooves commonly seen in *Au. afarensis* upper canines[10]. Its distal tubercle is also small and the mesial crown shoulder relatively short compared to the crown height and length of the mesial crest, thus it is less incisiform than *Au. afarensis* upper canines. It retains a more primitive, *Au. anamensis*-like condition in this regard.

The postcanine teeth of BRT-VP-3/1, particularly the P^4 and M^1, are very small (Fig. 4; see Extended Data Table 2 for summary statistics). The M^1 area of BRT-VP-3/1 is the smallest of all known Pliocene hominins (less *Ar. ramidus*), whereas the P^4 size is only approximated by A.L. 199-1, the smallest outlier in the *Au. afarensis* hypodigm. The M^2 also falls at the lower end of the *Au. afarensis* range and is slightly larger than that of KNM-WT 40000, the holotype of *K. platyops*. The P^4 to M^1 area ratio of BRT-VP-3/1 falls within the range of most Pliocene hominin taxa, but outside the range of *Paranthropus*. In terms of enamel thickness, the two-dimensional linear enamel thickness for the M^1 of BRT-VP-3/1 is similar to that of other early hominins such as *Au. afarensis*, *P. robustus* and *Au. africanus*. However, the two-dimensional and three-dimensional enamel thickness values for the M^2 of this specimen are high, most similar to *P. robustus* (see Supplementary Note 4 and Extended Data Tables 3 and 4 for details).

Although *Au. deyiremeda* and *K. platyops* show some similarities in maxillary morphology and molar size, they can be distinguished by a suite of qualitative characters related to the morphology of the nasoalveolar clivus, shape of the dental arcade, and morphology of the anterior maxillary dentition. The nasoalveolar clivus in *K. platyops* is flat both sagittally and transversely[3], whereas in *Au. deyiremeda* it is anteriorly convex in the transverse plane. In accordance with this difference, *Au. deyiremeda* and *K. platyops* differ in the shape of the anterior dental arcade. On the basis of the position of the preserved I^1 root, the transversely oblique orientation of the I^2 crown, and its placement relative to the canine and postcanine row, it is clear that the canine and incisors of BRT-VP-3/1 formed an arc with the incisor alveoli well anterior to the bi-canine line, as in *Au. afarensis* specimens such as A.L. 200-1a and A.L. 444-2 (ref. 9; see Extended Data Fig. 1f, g). In *K. platyops*, the incisors are arranged parallel to the bi-canine line as in *Paranthropus* and *Homo rudolfensis*[3]. *Kenyanthropus platyops* also has a derived low and curved zygomaticoalveolar crest[3], whereas this feature is not sufficiently developed to form a visible crest in BRT-VP-3/1. Instead, the lateral alveolar wall blends smoothly with the base of the zygomatic bone. Furthermore, computed tomography scans show that the incisor roots of BRT-VP-3/1 are straight and inclined posterosuperiorly, indicating procumbent incisors (Extended Data Fig. 1i, k). By contrast, the incisor roots of *K. platyops* do not show any sign of procumbency[3]. On the basis of root cross-section approximately 2 mm below the buccal cervicoenamel line of I^2, the I^1 root of BRT-VP-3/1 is also rounded and more robust than the mesiolaterally compressed I^2 root, unlike KNM-WT 40000 in which the I^1 and I^2 incisor roots are almost equal in size[3] (see Extended Data Fig. 1m). In general, *K. platyops* seems to be more derived than *Au. deyiremeda* in most of its maxillary and dental morphology.

The overall morphology of the paratype mandibles (BRT-VP-3/14 and WYT-VP-2/10; Fig. 1 and Extended Data Fig. 2) is comparable to that of eastern African robust taxa, although their overall size is within the range of *Au. afarensis*. The anterior origin of the ascending ramus at the posterior P_4 level is comparable to *P. boisei* mandibles such as the Peninj mandible and KGA-10-525 (ref. 14), and *P. robustus* specimens such as SK-12. *Australopithecus afarensis* mandibles have the origin of the ascending ramus high and more posterior, mostly distal to the first molar[9,15]. BRT-VP-3/14 and WYT-VP-2/10 have inflated mandibular corpora, especially at the M_{2-3} level, and they lack the lateral corpus hollow ubiquitous in *Au. afarensis* mandibles[9]. Corpus dimensions of BRT-VP-3/14 and WYT-VP-2/10 are notable because they are broader for their size than specimens assigned to *Au. afarensis* or early *Homo*. In this respect, they are more similar to *Paranthropus* (Fig. 5 and Supplementary Note 5). Mandibular specimens from Lomekwi whose taxonomic affinities have not been established with certainty (KNM-WT 8556 and KNM-WT 16006)[3,16], are described as having robust corpora with an ascending ramus take-off at P_4 and M_1, respectively. However, the robusticity of the Lomekwi specimens is not as pronounced as it is in WYT-VP-2/10 and BRT-VP-3/14. Furthermore, the KNM-WT 8556 premolars are derived: the P_3 has a well-developed metaconid and the P_4 is large and molarized[3]. By contrast, the P_3 of BRT-VP-3/14 is almost unicuspid, with only a trace of the metaconid, and the P_4 is not molarized.

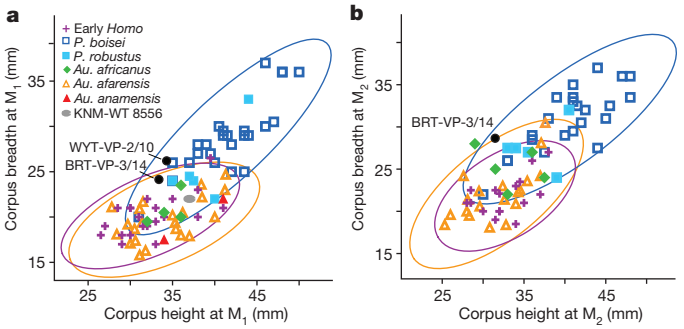

Figure 5 | Bivariate plots of mandibular corpus height and breadth among early hominins. **a**, Dimensions at the M_1 level. **b**, Dimensions at the M_2 level. The 95% confidence ellipses are shown for *Au. afarensis*, *P. boisei* and early *Homo* (see Supplementary Note 5 for details). The *Au. deyiremeda* corpora are relatively broad, comparable to *Paranthropus*. WYT-VP-2/10 falls outside the *Au. afarensis* ellipse at the M_1 level. BRT-VP-3/14 (represented by the mean of left and right sides) falls in an area of overlap at the M_1 level but at the edge of the *Au. afarensis* ellipse at the M_2 level. Mandibular measurements for the comparative taxa were taken from the references listed in Fig. 4 and ref. 14.

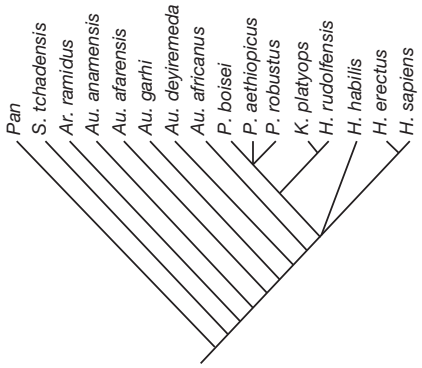

Figure 6 | Cladogram depicting the majority-rule consensus of 17 equally parsimonious trees that result from a phylogenetic analysis of the features preserved in the *Au. deyiremeda* hypodigm. Tree length = 63, consistency index = 0.63. The position of *Au. garhi* and topologies within the *Paranthropus* + *Kenyanthropus* + *Homo* clade are unstable when these features are considered. However, *Au. deyiremeda* is consistently placed as a sister taxon to a clade that includes *Au. africanus*, *Paranthropus*, and *Homo* (see Supplementary Notes 6–8 for further details).

The symphysis of BRT-VP-3/14 is thinner, superoinferiorly longer, and has a more receding external contour than that of WYT-VP-2/10 (Extended Data Fig. 2h, n). In the latter specimen, the superior half of the external contour is almost vertical but the inferior half is extremely receding similar to L.H.-4, the holotype of *Au. afarensis*[9,17,18]. Further similarities between WYT-VP-2/10 and L.H.-4 include the prominence of the superior and inferior transverse tori (hence the deep genioglossal fossa) and the posterior extension of the inferior transverse torus exceeding that of the superior transverse torus. BRT-VP-3/14 has weak transverse tori and a very shallow genioglossal fossa (similar to *Au. afarensis* specimens such as A.L. 333w-12 and A.L. 315-22) and a pronounced postincisive planum (comparable to A.L. 400-1). These differences are within the range of variation seen in *Au. afarensis* mandibles[9] and further show intra-taxon variability in mandibular symphyseal morphology. Although it was previously argued that two *Au. bahrelghazali* mandibles (KT 12 and KT 40) have symphyseal morphology that distinguishes them from *Au. afarensis* mandibles[5], they appear to also fall within the range of *Au. afarensis* variation[9,19,20].

In terms of the dentition, BRT-VP-3/14 has small premolars compared to *Au. afarensis* (see Extended Data Table 5 and Supplementary Note 5 for details). The small mandibular premolars appear to conform well with the small upper premolars and M^1 of BRT-VP-3/1. Despite the robust appearance of the mandible, the BRT-VP-3/1 maxilla is only slightly smaller when occluded with the BRT-VP-3/14 mandible (see Extended Data Fig. 5).

The 2.8-Myr-old early *Homo* mandible (LD 350-1) recently reported from Ledi–Geraru[21] is similar to *Au. deyiremeda* and some *Au. afarensis* specimens in its anterior corpus morphology. However, the derived features that are present in LD 350-1 and diagnostic of *Homo* are absent in the *Au. deyiremeda* mandibles (for example, posteriorly opening mental foramen, comparable anterior and posterior corpus height, M_3 mesiodistally shorter than M_2). Features of *Au. deyiremeda* that are derived relative to *Au. afarensis* and earlier hominins (for example, relatively robust mandibular corpus, anteriorly positioned root of the ascending ramus) are absent in LD 350-1 and other early *Homo* mandibles. Dentally, while the P_4 of BRT-VP-3/14 and LD 350-1 are comparable in size, the M_2 and M_3 of BRT-VP-3/14 are much larger (Extended Data Table 5).

Phylogenetic implications

The taxonomy and phylogenetic relationships among early hominins are becoming more complicated as new taxa are added to the Pliocene fossil record[2,3,22,23] and the temporal range and systematics of early *Homo* are reconsidered[21,24]. A phylogenetic analysis of the preserved morphological features of *Au. deyiremeda* fails to produce a single most-parsimonious cladogram. However, the results are fairly consistent in placing this species as a sister taxon to a clade including *Au. africanus*, *Paranthropus* and *Homo* (Fig. 6 and Supplementary Notes 6–8). There are many alternative phylogenies consistent with this topology, but the fact that *Au. deyiremeda* is positioned outside the *Paranthropus* and *Homo* clade implies that some features associated with one or both of these taxa are homoplastic. Therefore, the addition of *Au. deyiremeda* reinforces questions about dentognathic homoplasy in later Pliocene and early Pleistocene hominins.

There is now incontrovertible evidence to show that multiple hominins existed contemporaneously in eastern Africa during the Middle Pliocene[1,3]. Importantly, Woranso–Mille is geographically very close to Hadar (only 35 km north), where *Au. afarensis* is well documented. In combination, this suggests that multiple hominin species overlapped temporally and lived in close geographic proximity. What remains intriguing, and requires further investigation, is how these taxa are related to each other and to later hominins, and what environmental and ecological factors triggered such diversity. This has important implications for resource use and niche partitioning in Pliocene hominin palaeoecology, which can only be understood with the recovery and analysis of more hominin fossils and their associated fauna from Woranso–Mille and other contemporaneous sites.

Received 8 October 2014; accepted 9 April 2015.

1. Haile-Selassie, Y. *et al.* A new hominin foot from Ethiopia shows multiple Pliocene bipedal adaptations. *Nature* **483,** 565–570 (2012).
2. Brunet, M. *et al. Australopithecus bahrelghazali*, une nouvelle espèce d'Hominidé ancien de la région de Koro Toro (Tchad). *C. R. Acad. Sci.* **322,** 907–913 (1996).
3. Leakey, M. G. *et al.* New hominin genus from eastern Africa shows diverse middle Pliocene lineages. *Nature* **410,** 433–440 (2001).
4. Spoor, F., Leakey, M. G. & Leakey, L. N. Hominin diversity in the middle Pliocene of eastern Africa: the maxilla of KNM-WT 4000. *Phil. Trans. R. Soc. B* **365,** 3377–3388 (2010).
5. Guy, F. *et al.* Symphyseal shape variation in extant and fossil hominoids, and the symphysis of *Australopithecus bahrelghazali*. *J. Hum. Evol.* **55,** 37–47 (2008).
6. White, T. Early hominids – diversity or distortion? *Science* **299,** 1994–1997 (2003).
7. Lovejoy, C. O., Latimer, B., Suwa, G., Asfaw, B. & White, T. D. Combining prehension and propulsion: the foot of *Ardipithecus ramidus*. *Science* **326,** 72e1–72e8 (2009).
8. Kimbel, W. H., Johanson, D. C. & Rak, Y. Systematic assessment of a maxilla of *Homo* from Hadar, Ethiopia. *Am. J. Phys. Anthropol.* **103,** 235–262 (1997).
9. Kimbel, W. H., Rak, Y. & Johanson, D. C. *The Skull of* Australopithecus afarensis (Oxford Univ. Press, 2004).
10. Johanson, D. C., White, T. D. & Coppens, Y. Dental remains from the Hadar Formation, Ethiopia: 1974–1977 collections. *Am. J. Phys. Anthropol.* **57,** 545–603 (1982).
11. Ward, C. V., Leakey, M. G. & Walker, A. Morphology of *Australopithecus anamensis* from Kanapoi and Allia Bay, Kenya. *J. Hum. Evol.* **41,** 255–368 (2001).
12. Manthi, F., Plavcan, M. & Ward, C. New hominin fossils from Kanapoi, Kenya: mosaic evolution of canine evolution in early hominins. *So. Afr. J. Sci.* **108,** 1–9 (2012).
13. Ward, C. V., Manthi, F. K. & Plavcan, J. M. New fossils of *Australopithecus anamensis* from Kanapoi, West Turkana, Kenya (2003–2008). *J. Hum. Evol.* **65,** 501–524 (2013).
14. Suwa, G. *et al.* The first skull of *Australopithecus boisei*. *Nature* **389,** 489–492 (1997).
15. Kimbel, W. H. & Delezene, L. K. 'Lucy' redux: a review of research on *Australopithecus afarensis*. *Am. J. Phys. Anthropol.* **49,** 2–48 (2009).
16. Brown, B., Brown, F. H. & Walker, A. New hominids from the Lake Turkana Basin, Kenya. *J. Hum. Evol.* **41,** 29–44 (2001).
17. White, T. D. & Johanson, D. C. Pliocene hominid mandibles from the Hadar Formation. Ethiopia: 1974–1977 collections. *Am. J. Phys. Anthropol.* **57,** 501–544 (1982).
18. Johanson, D. C., White, T. & Coppens, Y. *A New Species of the Genus* Australopithecus *(Primates: Hominidae) From the Pliocene of Eastern Africa (*Kirtlandia*)* (Cleveland Museum of Natural History, 1978).
19. White, T. D., Suwa, G., Simpson, S. W. & Asfaw, B. Jaws and teeth of *Australopithecus afarensis* from Maka. Middle Awash, Ethiopia. *Am. J. Phys. Anthropol.* **111,** 45–68 (2000).
20. Wood, B. & Richmond, B. Human evolution: taxonomy and paleobiology. *J. Anat.* **197,** 19–60 (2000).
21. Villmoare, B. *et al.* Early *Homo* at 2.8 Ma from Ledi-Geraru, Afar, Ethiopia. *Science* **347,** 1352–1355 (2015).
22. Asfaw, B. *et al. Australopithecus garhi*: a new species of early hominid from Ethiopia. *Science* **284,** 629–635 (1999).
23. Leakey, M. G., Feibel, C. S., McDougall, I. & Walker, A. New four-million-year-old hominid species from Kanapoi and Allia Bay, Kenya. *Nature* **376,** 565–571 (1995).

24. Spoor, F. *et al.* Reconstructed *Homo habilis* type OH 7 suggests deep-rooted species diversity in early *Homo. Nature* **519,** 83–86 (2015).
25. Wood, B. *Koobi Fora Research Project* Vol. 4 (Clarendon, 1991).
26. White, T. D., Johanson, D. C. & Kimbel, W. H. in *New Interpretations of Ape and Human Ancestry* (eds Ciochon, R. L. & Corruccini, R. S.) 721–780 (Plenum, 1983).
27. Harrison, T. in *Paleontology and Geology of Laetoli: Human Evolution in Context* (ed. Harrison, T.) Vol. 2 141–188 (Dordrecht: Springer, 2011).
28. White, T. D. Additional fossil hominids from Laetoli, Tanzania: 1976–1979 specimens. *Am. J. Phys. Anthropol.* **53,** 487–504 (1980).
29. White, T. D. New fossil hominids from Laetolil, Tanzania. *Am. J. Phys. Anthropol.* **46,** 197–229 (1977).
30. White, T. D. *et al.* Asa Issie, Aramis and the origin of *Australopithecus. Nature* **440,** 883–889 (2006).
31. White, T. D., Suwa, G., Simpson, S. W. & Asfaw, B. Jaws and teeth of *Australopithecus afarensis* from Maka. Middle Awash, Ethiopia. *Am. J. Phys. Anthropol.* **111,** 45–68 (2000).
32. Suwa, G. *et al.* Paleobiological implications of the *Ardipithecus ramidus* dentition. *Science* **326,** 94–99 (2009).
33. Leakey, M. G. *et al.* New fossils from Koobi Fora in northern Kenya confirm taxonomic diversity in early *Homo. Nature* **488,** 201–204 (2012).
34. Olejniczak, A. J. *et al.* Three-dimensional molar enamel distribution and thickness in *Australopithecus* and *Paranthropus. Biol. Lett.* **4,** 406–410 (2008).

Supplementary Information is available in the online version of the paper.

Acknowledgements We thank the Authority for Research and Conservation of Cultural Heritage and the Afar Regional State of Ethiopia for permission to conduct field and laboratory research, the Afar people of the Woranso–Mille area for their hospitality, and the project's fieldwork crew members for their incredible contributions in our fieldwork endeavours. We would also like to thank S. W. Simpson and W. H. Kimbel for their constructive comments and discussions throughout the preparation of this manuscript; G. Suwa, T. White and B. Asfaw for access to the original *Ardipithecus ramidus* material; W. H. Kimbel for access to the original *Australopithecus afarensis* material; F. Spoor for discussion of *Kenyanthropus platyops* morphology and Lomekwi mandibular metrics; D. F. Su for comments and assistance with the figures. This research was financially supported by grants from the LSB Leakey Foundation, the National Geographic Society, the Cleveland Museum of Natural History, and the National Science Foundation (BCS-0234320, BCS-0321893, BCS-0542037, BCS-1124705, BCS-1124713, BCS-1124716, BCS-1125157 and BCS-1125345).

Author Contributions Y.H.-S. directed the field research. A.D., B.Z.S., M.A., L.G. and S.M.M. participated in the field research. T.M.R. conducted the computed tomography scanning and made the virtual reconstructions. A.D., B.Z.S., L.G. and M.A. studied the geological context, while L.G. and G.S. conducted the palaeomagnetic analysis. S.M.M. conducted the phylogenetic analysis. Y.H.-S. and S.M.M. made comparative observations and carried out analyses. Y.H.-S. took the lead in writing the paper with contributions from all coauthors.

Author Information The LSID urn:lsid:zoobank.org:pub:0C492889-01AC-4CDD-96FD-0E08A51F3CBB has been deposited in ZooBank. Reprints and permissions information is available at www.nature.com/reprints. The authors declare no competing financial interests. Readers are welcome to comment on the online version of the paper.
Correspondence and requests for materials should be addressed to Y.H.-S. (yhailese@cmnh.org).

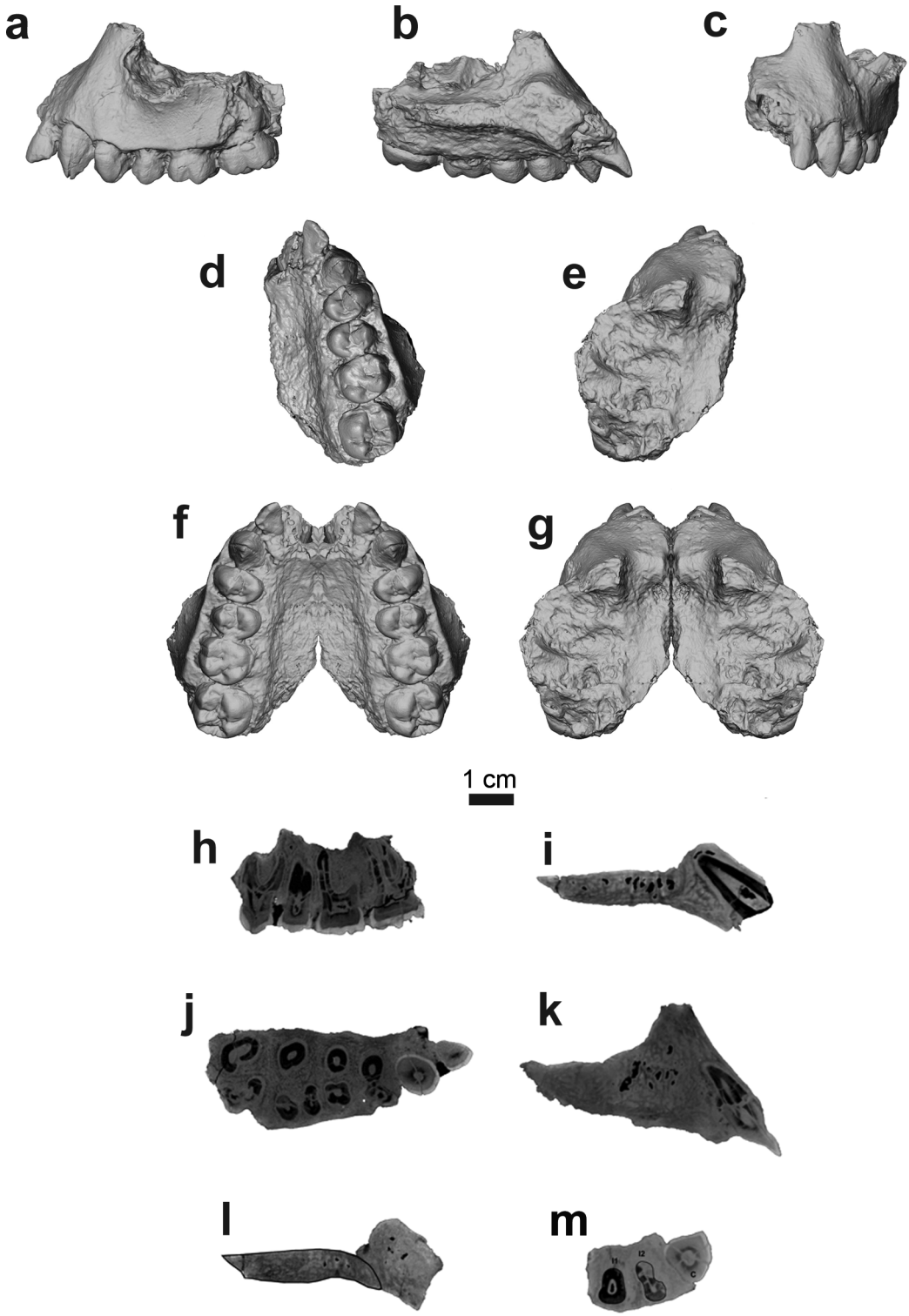

Extended Data Figure 1 | Computed-tomography-based visualization of BRT-VP-3/1. **a**, Lateral view. **b**, Medial view. **c**, Anterior view. **d**, Palatal view. **e**, Superior view. **f**, Palatal view mirror-imaged on midline. **g**, Superior view mirror-imaged on midline. Computed-tomography-based cross-sections of BRT-VP-3/1. **h**, Sagittal cross-section along the centre of the dental row showing root morphology. **i**, Sagittal cross-section at I^1. **j**, Transverse cross-section along the roots showing the number of roots of each tooth. **k**, Sagittal cross-section at I^2. **l**, Midsagittal cross-section showing the shape of the palatine process and nasoalveolar clivus. **m**, Transverse cross-section across the incisors and the canine.

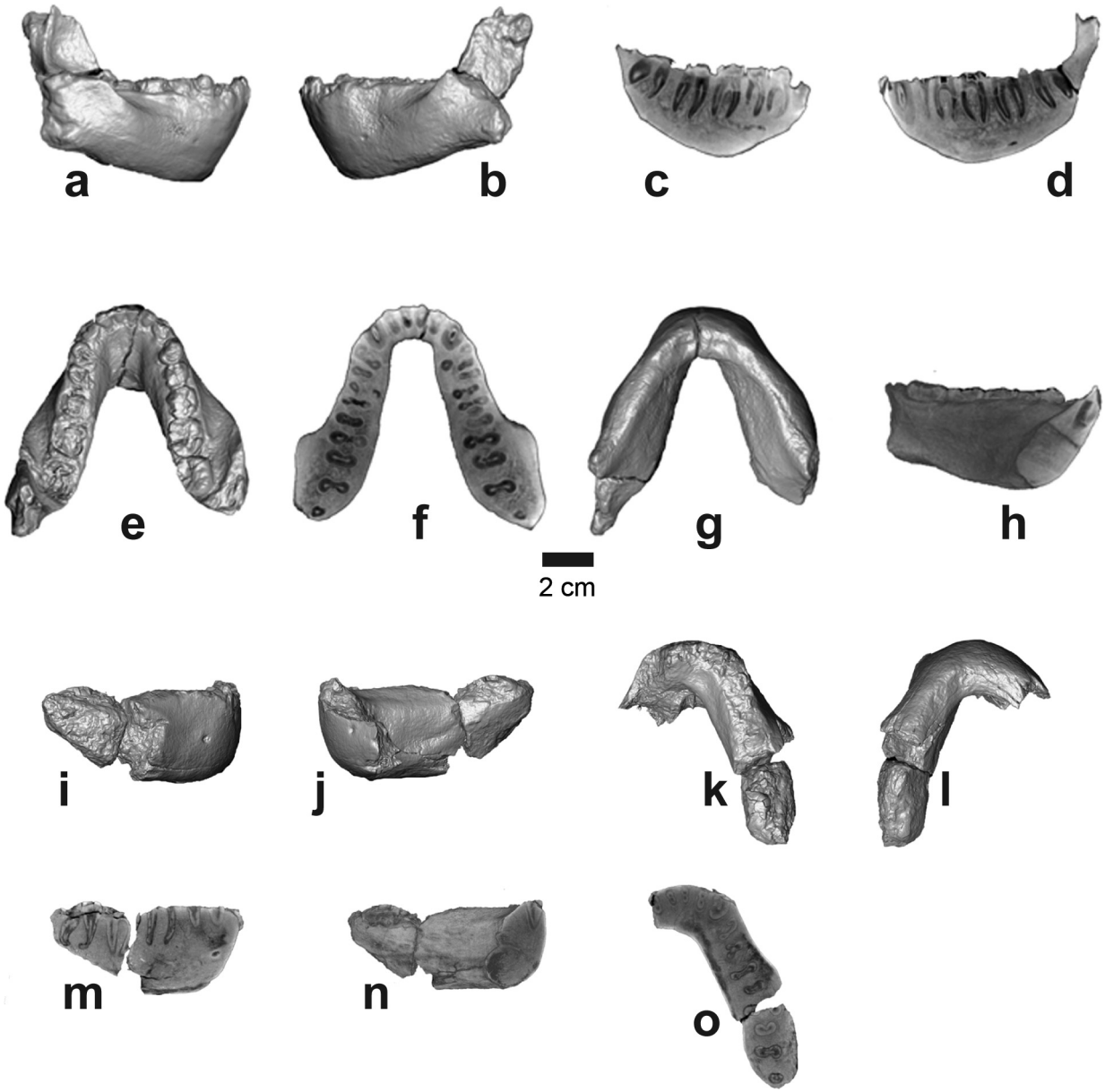

Extended Data Figure 2 | Computed-tomography-based visualization of BRT-VP-3/14. **a**, Right lateral view. **b**, Left lateral view. **c**, Sagittal cross-section along the centre of the right dental row showing root morphology. **d**, Sagittal cross-section along the centre of the left dental row showing root morphology. **e**, Occlusal view. **f**, Transverse cross-section along the roots showing the number of roots of each tooth. Note that the premolars have several roots. **g**, Basal view. **h**, Symphyseal cross-section. Computed-tomography-based visualization of WYT-VP-2/10. **i**, Right lateral view. **j**, Medial view. **k**, Occlusal view. **l**, Basal view. **m**, Sagittal cross-section along the centre of the dental row showing root morphology. **n**, Symphyseal cross-section. **o**, Transverse cross-section along the roots showing the number of roots of each tooth.

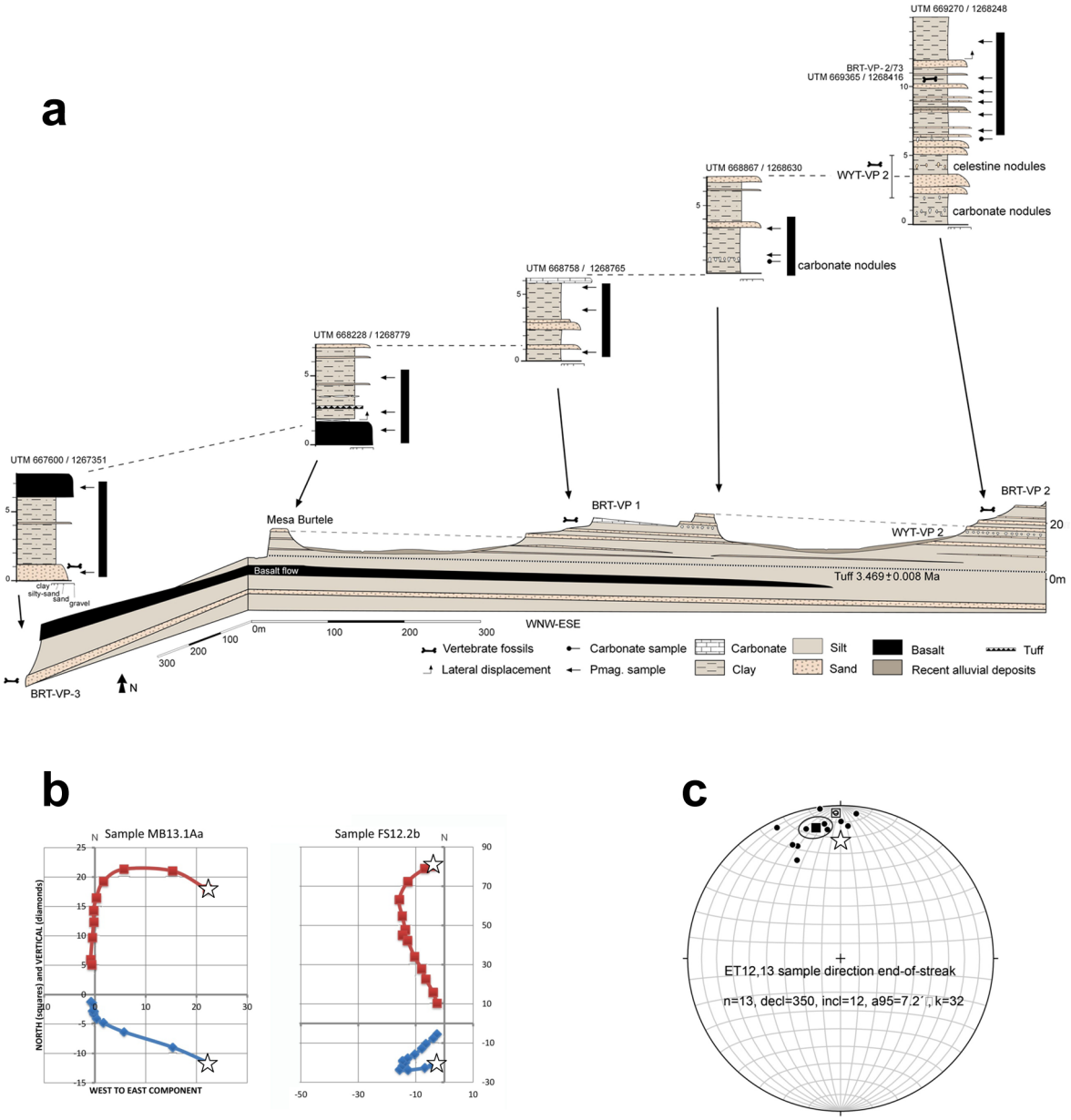

Extended Data Figure 3 | Magnetostratigraphy. **a**, Magnetostratigraphy for the Burtele area, measured in five subsections beginning with the oldest strata in the southwest (BRT-VP-3), to the youngest at BRT-VP-2 (see Fig. 2 for subsections locations). This stratigraphy consists predominantly of claystones/siltstones alternating with sandstones, and includes a 20-cm carbonate bed, a 2–6-m basalt flow, and a 5-cm tuff bed. The sandstones occupy slightly sinuous fluvial channels with a low width/depth ratio in a weakly confined setting. The sandstone beds are continuous and interestratified with pedogenically modified fine-grained overbank and ephemeral lake deposits. The proportion of sandstones increases upwards in the section, where it is accompanied by the occurrence of celestine nodules indicating increased aridity. Sixteen palaeomagnetic samples were obtained from fine-grained lithologies. All samples demonstrate normal polarity (black bars), interpreted as belonging to a single polarity chron C2An.3n (3.596–3.330 Myr old) of the Astronomically Tuned Neogene Time Scale (ATNTS2004). **b**, Orthogonal demagnetization diagrams showing vector endpoints after alternating field and thermal demagnetization for samples MB13.1Aa and FS12.2b. Horizontal projections are shown as squares, vertical projection as diamonds, and NRM (4 mT) starting point as star. **c**, Palaeomagnetic directions for the Burtele stratigraphy from samples collected a long different stratigraphic horizons. Stereographic projection referenced to magnetic North (declination 2° E), with solid symbols on lower hemisphere (plus inclination). Represented directions are the mean directions for each sample from three specimens. The start shows the location of the expected normal direction for this latitude (000/22).

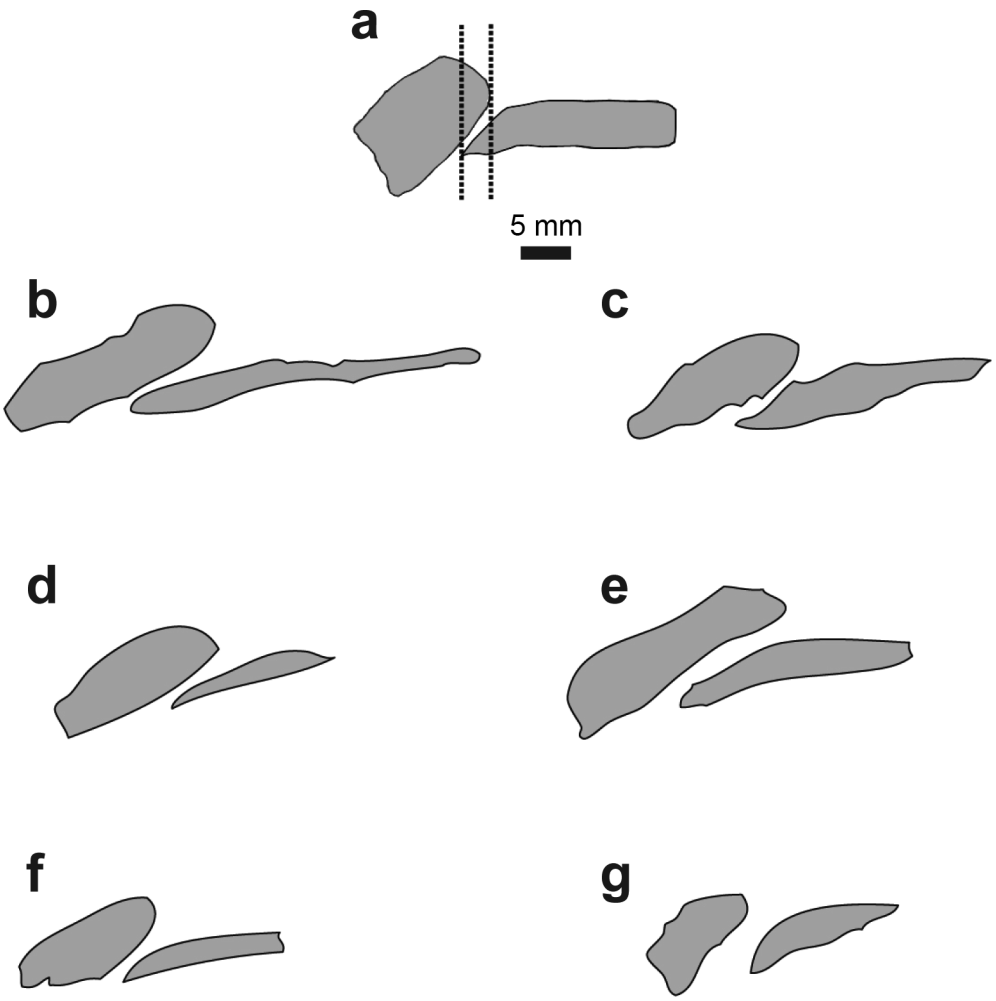

Extended Data Figure 4 | Comparisons of midsagittal cross section of the hard palate and nasoalveolar clivus. **a**, BRT-VP-3/1. **b**, A.L. 444-2. **c**, A.L. 200-1. **d**, A.L. 486-1. **e**, A.L. 427-1. **f**, A.L. 199-1. **g**. A.L. 442-1. Note that the overlap between the hard palate and the nasolalveolar clivus of BRT-VP-3/1 is small relative to most *Au. afarensis* specimens. Midsagittal cross-sections of *Au. afarensis* maxillae were modified from Fig. 5.22 in ref. 9.

Extended Data Figure 5 | BRT-VP-3/1 (reversed) and BRT-VP-3/14 shown in occlusion. The upper canine is aligned mesial to the P_3. Despite the apparently large size of the mandible (BRT-VP-3/14), the maxilla (BRT-VP-3/1) is only slightly smaller. The position of the second molars is indicated to show that the canine-to-second-molar length is comparable in both specimens.

Extended Data Table 1 | Measurements of the paratype mandibles

	Measurement	BRT-VP-3/14	WYT-VP-2/10
1	Symphyseal height	42.2	40.7
2	Maximum symphyseal depth	19.9	23.3
3	Horizontal position of mental foramen	P3/P4	P3
4	Mental foramen height from base	19.4	18
5	Mental foramen height from alveolar margin	~17.4	~16.6
6	Corpus height at P_4	36.6, 35.8	35.7
7	Corpus width at P_4	21.1, 21.8	23.8
8	Corpus height at P_4/M_1	36.3, 35.9	34.8
9	Corpus width at P_4/M_1	22.8, 22.7	27.11
10	Corpus height at M_1	33.8, 33.0	34.3
11	Corpus width at M_1	24.5, 23.6	26.2
12	Corpus height at M_1/M_2	33.3, 31.9	-
13	Corpus width at M_1/M_2	25.3, 28.0	-
14	Corpus height at M_2	32.4, 30.5	-
15	Corpus width at M_2	28.2, 29	-
16	Corpus height at M_2/M_3	30.8, 28.5	-
17	Corpus width at M_2/M_3	28.1, 29.5	-
18	P_4-P_4 distance at mid-crown on lingual side	29.9	-
19	M_1-M_1 distance at mid-crown on lingual side	~33.5	-

Corpus dimensions of BRT-VP-3/14 are reported for both right and left sides. Measurements 1–5 were taken following the methods used in ref. 25. Measurements 6–19 were taken following the methods used in ref. 17. All measurements are in millimetres.

Extended Data Table 2 | Statistical summary of measurements of early hominin maxillae and upper dentition

		Subnasal Angle	Palate Depth	C^1 MD	$\sqrt{P^4}$ Area	$\sqrt{M^1}$ Area	$\sqrt{M^2}$ Area	$\sqrt{P^4}$ Area / $\sqrt{M^1}$ Area
BRT-VP-3/1		~39	~13.4	8.3	9.1	10.8	12.5	0.84
Au. anamensis	n	1	—	2	4	8	10	4
	mean	27	—	10.8	10.6	12.5	13.7	0.90
	range	—	—	9.9 - 11.7	9.7 - 12.1	11.0 - 13.1	12.3 - 15.5	0.79 - 0.92
	s.d.	—	—	—	1.0	0.74	1.02	0.06
Au. afarensis	n	6	6	10	15	11	12	11
	mean	34.6	11.3	9.9	10.6	12.9	13.9	0.81
	range	29 - 39	8.5 - 14	8.9 - 11.6	9.2 - 12.5	11.4 - 14.2	12.3 - 14.9	0.74 - 0.97
	s.d.	3.5	1.8	0.74	0.72	0.88	0.73	0.07
K. platyops	n = 1	47	—	—	—	—	11.9	—
Au. garhi	n = 1	27	—	11.6	—	—	—	—
Au. africanus	n	9	2	5	9	12	14	4
	mean	34.2	16.3	9.6	11.3	13.2	14.6	0.87
	range	30 - 37	14.5 - 18.0	8.8 - 10.0	10.8 - 12.4	12.4 - 14.4	13.3 - 16.4	0.84 - 0.89
	s.d.	1.9	—	0.48	0.50	0.50	0.95	0.02
early *Homo*	n	—	—	7	12	18	17	9
	mean	—	—	9.4	10.5	12.7	13.3	0.81
	range	—	—	8.3 - 11.5	9.7 - 12.1	11.4 - 14.5	12.5 - 16.0	0.77 - 0.88
	s.d.	—	—	1.35	0.68	0.84	0.96	0.03
P. aethiopicus	n	2	1	—	—	—	—	—
	mean	34	15	—	—	—	—	—
	range	31 - 37	—	—	—	—	—	—
	s.d.	—	—	—	—	—	—	—
P. robustus	n	8	5	13	18	19	16	7
	mean	36.8	13.8	8.5	12.7	14.1	15.2	0.89
	range	32 - 39	12.2 - 15.5	7.6 - 9.2	11.4 - 14.0	13.3 - 15.3	14.0 - 16.3	0.88 - 0.97
	s.d.	4.1	1.4	0.43	0.65	0.43	0.64	0.04
P. boisei	n	2	3	8	6	12	11	6
	mean	35.9	21	8.6	14.0	15.3	16.4	0.93
	range	33 - 39	20 - 22	6.5 - 10.8	13.5 - 14.6	13.3 - 16.4	15.6 - 19.0	0.89-0.94
	s.d.	—	1.0	1.18	0.54	1.02	1.43	0.02

Canine comparative measurements are taken from refs 13, 22, 23 and 26. Subnasal angle comparative measurements are taken from summary data compiled in ref. 4. Palate depth comparative measurements are from refs 3 and 27. All other data for the comparative taxa were compiled from refs 3, 23, 25, 28–33. Subnasal angle is measured as the subnasal clivus (nasospinale-prosthion) to the postcanine alveolar margin. Palate depth is measured at M^1/M^2 for all specimens, except for *P. aethiopicus* (EP 1500/01), which was measured at P^3/P^4 (but appears to retain a constant depth posteriorly[27].

Extended Data Table 3 | Enamel thickness measurements

MicroCT scan settings							
Fossil	**Energy Settings**	**Field of View (mm)**	**x, pixel size (mm)**	**z slice thickness (mm)**			
BRT-VP-3/1	180 kV, 0.250 mA	43.01	0.042	0.046			
BRT-VP-3/14	250 kV, 2.0 mA	131.69	0.129	0.129			
WYT-VP-2/10	250 kV, 1.0 mA	77.86	0.076	0.074			
BRT-VP-3/1 Two-dimensional enamel thickness							
	Cusp tip thickness (mm)		**Maximum occlusal thickness (mm)**		**Maximum lateral thickness (mm)**		**Crown Area (mm^2)**
	Buccal	*Lingual*	*Buccal*	*Lingual*	*Buccal*	*Lingual*	
M^1	too worn	too worn	1.11	1.03	1.2	1.38	11.03
M^2	1.76	1.93	1.53	1.66	1.71	2.15	12.36
BRT-VP-3/1 Three-dimensional enamel thickness							
	Enamel Volume (mm^3)	**Dentine area (mm^2)**	**Dentine volume (mm^3)**	**AET (average enamel thickness)**	**AETSTD (AET standardized)**		
M^2 3D	325.357	186.478	273.224	1.745	26.89		

MicroCT scan settings, two-dimensional and three-dimensional enamel thickness measurements for BRT-VP-3/1.

Extended Data Table 4 | Three-dimensional and two-dimensional average and relative enamel thicknesses

	BRT-VP-3/1 M^2	*Homo sapiens*	*P. robustus*	*A. africanus*	*H. neanderthalensis*	*Pongo pygmaeus*	*Pan troglodytes*	*Gorilla gorilla*
3D Sample	1	39	9	9	29	12	26	9
Enamel volume (mm^3)	325.36	218.91	557.51	478.85	225.47	197.91	137	372.01
Dentine volume (mm^3)	186.48	226.83	507.6	598.9	345.65	336.05	166.05	1023.18
EDJ surface area (mm^2)	273.22	162.56	311.8	332.67	53.8	199.75	116.21	375.89
3D AET (mm)	1.74	1.43	1.83	1.48	1.08	1.01	0.75	0.98
3D RET	26.89	23.97	23.27	17.7	15.55	14.49	11.8	9.77
2D Sample	1	257	9	9	42	41	40	15
Enamel area (mm^2)	24.76	24.19	44.75	36.2	21.97	23.42	14.63	29.37
Dentine area (mm^2)	28.83	38.73	53.23	52.27	41.65	50.93	36.95	79.29
EDJ length (mm)	17.38	19.6	21.87	22.42	20.75	21.34	19.47	28.25
2D AET (mm)	1.42	1.22	2.03	1.63	1.06	1.1	0.75	1.04
2D RET	34.17	20.06	28.38	22.79	16.44	15.49	13.23	11.68

The values for the BRT-VP-3/1 M^2 are compared with extinct hominins and extant hominoids. Data for fossil hominins and hominoids taken from ref. 34. AET, average enamel thickness; EDJ, enamel–dentine junction; RET, relative enamel thickness.

Extended Data Table 5 | Mandibular dental dimensions (P_3–M_3) and robusticity indices (at the M_1 and M_2 levels) of *Au. deyiremeda* and other Plio-Pleistocene hominins

		P_3		P_4		M_1		M_2		M_3		Robusticity Index at M_1	Robusticity Index at M_2
		MD	BL	MD	BL	MD	BL	MD	BL	MD	BL		
BRT-VP-3/14	n = 1	7.6	10.8	8.2	10.6	(12.6)	(12.6)	(14.8)	(13.8)	(15.8)	(13.4)	0.72	0.91
WYT-VP-2/10	n = 1	-	-	-	-	-	-	-	-	-	-	0.76	-
KNM-WT 8556	n = 1	9.9	12.2	11.4	12.8	13.6	13.1	-	(15.0)	(19.0)	-	(0.59)	-
LD 350-1	n = 1	-	-	8.7	10.5	(12.2)	-	13.2	12.5	13.0	12.2	(0.61)	(0.69)
Au. anamensis	n	6	5	6	7	8	8	7	7	7	7	2	-
	mean	9.9	10.9	9.0	10.6	12.6	11.7	14.3	13.5	15.0	13.2	0.53	-
	range	9.3 - 10.9	9.5 - 12.0	7.4 - 9.8	9.6 - 11.9	11.6 - 13.7	10.2 - 13.3	13.0 - 15.9	12.3 - 14.9	13.7 - 17.0	12.1 - 13.7	0.51 - 0.54	-
	s.d	0.60	1.00	0.95	0.84	0.87	1.10	0.92	0.88	1.17	0.66	-	-
Au. afarensis	n	29	29	26	22	31	24	33	31	26	23	22	19
	mean	9.5	10.7	9.8	11.0	13.1	12.6	14.3	13.5	15.2	13.4	0.58	0.7
	range	7.9 - 12.6	8.9 - 13.6	7.7 - 11.4	9.8 - 11.8	10.1 - 14.8	11.0 - 13.9	12.1 - 16.5	11.1 - 15.2	13.4 - 18.1	11.3 - 15.3	0.48 - 0.76	0.56 - 0.88
	s.d	1.00	1.10	1.00	0.84	0.90	0.80	1.20	1.00	1.30	1.00	0.07	0.08
Au. africanus	n	18	17	24	20	32	30	37	40	34	31	4	5
	mean	9.7	11.4	10.4	11.6	13.9	13.2	15.7	14.4	16.1	14.5	0.61	0.76
	range	8.4 - 11.2	9.2 - 13.9	9.3 - 12.3	10.3 - 13.4	12.4 - 15.8	10.8 - 15.1	14.0 - 17.8	12.7 - 16.8	12.9 - 18.5	12.1 - 16.8	0.56 - 0.65	0.64 - 0.97
	s.d	0.74	1.17	0.76	0.90	1.07	0.90	0.98	0.99	1.10	1.08	0.04	0.13
Early *Homo*	n	12	11	9	9	15	16	14	15	12	12	22	16
	mean	10.0	10.4	10.5	10.9	14.1	12.2	15.5	13.6	15.4	13.0	0.63	0.67
	range	8.9 - 11.1	8.0 - 12.3	9.1 - 11.8	8.1 - 12.7	13.0 - 15.6	10.6 - 14.1	13.9 - 18.3	11.7 - 15.4	14.0 - 17.5	11.7 - 14.7	0.51 - 0.74	0.54 - 0.79
	s.d	0.71	1.36	0.90	1.42	0.89	0.94	1.28	1.07	0.96	0.94	0.06	0.07
P. robustus	n	20	19	17	16	24	18	20	20	22	21	5	5
	mean	10.2	11.6	11.5	13.1	14.7	13.7	16.3	14.7	17.1	14.5	0.66	0.76
	range	9.0 - 11.4	9.0 - 13.7	10.6 - 12.6	11.5 - 14.8	13.2 - 16.5	11.8 - 15.0	14.8 - 17.9	12.8 - 16.3	15.1 - 20.5	12.6 - 17.0	0.55 - 0.75	0.62 - 0.83
	s.d	0.61	1.14	0.62	1.11	0.77	0.85	0.90	0.84	1.38	1.14	0.07	0.08
P. boisei	n	5	5	9	9	10	6	8	6	9	12	25	23
	mean	11.1	13.0	13.5	14.3	16.5	15.5	18.2	16.9	16.4	20.0	0.69	0.76
	range	8.9 - 13.0	11.4 - 13.7	10.1 - 15.6	12.3 - 16.5	15.4 - 18.6	14.4 - 17.6	16.4 - 20.0	15.8 - 18.6	14.7 - 19.2	17.6 - 22.4	0.57 - 0.80	0.63 - 0.86
	s.d	1.66	0.93	1.76	1.28	0.97	1.17	1.33	1.11	1.56	1.71	0.05	0.06

The values reported for BRT-VP-3/14 are averages of the left and right sides. The data for LD 350-1 are taken from ref. 21 and corrected for interproximal wear. Summary statistics for the comparative taxa were taken from ref. 15 and the references listed in Extended Data Table 2. Values in parentheses are estimates or corrected for breakage and/or interproximal attrition.